Fokker-Planck Linearization for non-Gaussian Stochastic Elastoplastic Finite Elements

Konstantinos Karapiperis[a,*], Kallol Sett[b], Levent M. Kavvas[a], Boris Jeremič[a,c]

[a]*Department of Civil and Environmental Engineering, University of California, Davis, CA, USA*
[b]*Department of Civil, Structural and Environmental Engineering, University at Buffalo, The State University at New York, Buffalo, NY, USA*
[c]*Earth Science Division, Lawrence Berkeley National Laboratory, Berkeley, CA, USA*

Abstract

Presented here is a finite element framework for the solution of stochastic elastoplastic boundary value problems. The elastic/linearized part is based on a non-Gaussian stochastic Galerkin formulation, where the stiffness random field is decomposed using Polynomial Chaos expansion. In the constitutive level, a Fokker-Planck-Kolmogorov (FPK) plasticity framework is utilized. A linearization procedure is developed that serves to update the Polynomial Chaos coefficients of the expanded random stiffness in the elastoplastic regime, leading to a nonlinear least-squares optimization problem. The proposed framework is illustrated in a static shear beam example of elastic-perfectly plastic as well as isotropic hardening material.

Keywords: Fokker-Planck equation, Elastoplasticity, Stochastic Finite Elements, Linearization, Polynomial Chaos

*Corresponding author

1. Introduction

So far, in constitutive modeling, material parameters have been defined in a deterministic fashion by usually extracting the mean from a number of experiments. However, the behavior of all engineering materials, let alone geomaterials, is inherently uncertain, as portrayed by various researchers [1–3]. The uncertain response follows from inherent uncertainty of material behavior or spatial non-uniformity of material distribution. In addition, the nonlinear material behavior present in several engineering applications is usually described using elastoplastic constitutive relations. The physical or phenomenological components of such a model are ideally described by random fields, most of which are non-Gaussian. Modeling them as Gaussian fields can induce both inaccuracy and instability to the solution of a boundary value problem. For example, a Gaussian representation of the material stiffness results in inaccurate higher order moments while physically allowing negative realizations of the process to occur (softening). To realistically approximate such a physical quantity, a strictly positive definite field is required.

It is generally accepted that intrusive uncertainty quantification (UQ) frameworks, in which the uncertainty is propagated through the governing differential equations, are more efficient than non-intrusive ones. However, most researchers have focused on non-intrusive methods, which are easier to develop and utilize existing computational tools, or have limited their attention to intrusive UQ for simpler problems. The simplest example of a non-intrusive method is Monte Carlo Simulation (MCS) [4, 5], which may be seen as a direct integration method in which the integration points are chosen randomly over the probability space. Depending on the application, the latter approach can prove so computationally demanding that any practical application is hindered, at least for elasto-plastic models. Lately, more sophisticated sampling-based approaches have been developed including stochastic collocation [6, 7] and non-intrusive Galerkin techniques [8]. The applicability of those methods is not affected by the complexity of the problem since they act as wrappers on a deterministic solver which in turn acts as a "black box".

Several researchers have dealt so far with intrusive uncertainty quantification in computational mechanics with an emphasis in linear problems. A comprehensive review of such methods may be found in Matthies et al. [5], Keese [9], Matthies [10], where the authors also provide insight to the well-posedness and structure of a stochastic boundary value problem. So far, the most popular method for the quantification of uncertainty has been the Stochastic Finite Element Method (SFEM) [11], which relies on a spectral decomposition of parametric uncertainties and a Polynomial Chaos [12] approximation of the output random field. It is one of the first developments of a stochastic Galerkin method, where the problem is formulated in a variational form and holds in a weak sense. This class of methods allows an explicit functional representation of the solution in terms of independent random variables. An overview of stochastic Galerkin methods may be found in [10, 13, 14]. The curse of dimensionality associated with these methods is one of the topics that researchers have attempted to address lately. Xiu and Karniadakis [15] introduced the generalized Polynomial Chaos expansion which guarantees optimum (exponential) convergence rates for different classes of non-Gaussian processes. An optimum basis from the Askey family of orthogonal polynomials was utilized which reduces the dimensionality of the system. Other researchers have focused on developing sparse approximations by applying low-rank tensor product techniques [16], proper generalized decompositions and separated representations [17].

The first attempt to extend SFEM to nonlinear material behavior was by Anders and Hori [18], who used a perturbation expansion at the stochastic mean behavior. In computing the mean behavior they took advantage of bounding media approximation by introducing two fictitious bounding bodies providing an upper and a lower bound for the mean. This method, however, inherits the ”closure problem” (essentially the need for higher order statistical moments in order to calculate lower order statistical moments) and suffers from the ”small coefficient of variation” requirement for the material parameters. Later, Jeremić et al. [19] derived a second-order exact expression for the evolution of the probability density function of stress for elastoplastic constitutive rate equations with uncertain material parameters. Utilizing an Eulerian-Lagrangian form of the Fokker-Planck equation [20], the aforementioned ”closure problem” associated with regular perturbation methods is resolved. Afterwards, Jeremić [21] modified their approach to account for probabilistic rather than expected yielding and incorporated their developed FPK-based elastoplastic model in a Gaussian spectral stochastic finite element framework [22]. Finally, Rosić [23] presented in detail the variational theory behind the mixed-hardening stochastic plasticity problem along with stochastic versions of relevant established computational plasticity algorithms.

In this paper, we utilize a Fokker-Planck-Kolmogorov plasticity framework at the constitutive level and a stochastic Galerkin framework at the finite element level. Non-Gaussian parametric uncertainty is considered through a combined Karhunen-Lo ‘eve/Polynomial Chaos (KL/PC) expansion. The above are coupled through an FPK linearization scheme that updates the coefficients of the polynomial chaos (PC) approximation of the random stiffness. This method may be tailored to provide varying order of accuracy counterbalanced by computational efficiency by appropriately choosing the KL/PC spaces in which the constitutive integration procedure is performed. First, the stochastic approximation schemes are discussed followed by the finite element formulation. Next, the underlying Fokker-Planck-Kolmogorov framework is introduced along with the proposed linearization procedure and the complete framework illustrated in a simple static shear beam example.

2. Stochastic discretization

2.1. Elastic stiffness

Any arbitrary non-stationary stiffness random field may be approximated using a combined Karhunen-Lo ‘eve/Polynomial Chaos methodology. This technique involves evaluation of an arbitrary stochastic process as a polynomial of a suitable underlying Gaussian field, whose covariance structure is characterized by means of the Karhunen-Lo ‘eve expansion (KLE). Following Sakamoto and Ghanem [24], we represent the uncertain elastic constitutive tensor field with the help of the polynomial chaos expansion (PCE):

$$D(\mathbf{x}, \theta) = \sum_{i=0}^{M} r_i(x)\Phi_i[\{\xi_r(\theta)\}] \tag{1}$$

where $\Phi_i[\{\xi_r(\theta)\}]$ is a set of Hermite polynomials of an underlying Gaussian set $\xi_r(\theta)$. It can be shown that the PCE is convergent in $L_2(\Omega)$ where Ω denotes the space of the random variables. A relevant convergence rate study can be found in [25].

The spatially dependent coefficients r_i may be computed via simple projection but this kind of expansion is defined without any reference to the random field $D(\mathbf{x}, \theta)$ and the expected accuracy is low. Therefore, a correlation structure is endowed to the underlying field by considering the following representation:

$$D(\mathbf{x}, \theta) = \sum_{i=0}^{M} D_i(\mathbf{x})\Gamma_i[\mathbf{x}, \theta)] \tag{2}$$

where $\Gamma_i[\mathbf{x}, \theta]$ is now a set of Hermite polynomials of an underlying correlated Gaussian field $\gamma(\mathbf{x}, \theta)$. The orthogonality of the polynomials is employed to calculate the coefficients $D_i(\mathbf{x})$ as:

$$D_i(\mathbf{x}) = \frac{\langle D\Gamma_i \rangle}{\langle \Gamma_i^2 \rangle} \tag{3}$$

where the numerator can be evaluated using some type of numerical quadrature, for example Monte Carlo (MC) or Quasi Monte Carlo (QMC) techniques. The correlation function of $\gamma(\mathbf{x}, \theta)$ induced on $D(\mathbf{x}, \theta)$ is given as the solution to the following polynomial equation [24]:

$$\rho_D(\mathbf{x}_1, \mathbf{x}_2) = \sum_{i=1}^{M} D_i(\mathbf{x}_1) D_i(\mathbf{x}_2) i! \, \langle \gamma(\mathbf{x}_1)\gamma(\mathbf{x}_2) \rangle^i \tag{4}$$

This equation is solved by discretizing the domain into a number of nodes and solving the resulting system of equations. Knowing the above, the correlated random field $\gamma(\mathbf{x}, \theta)$ may be expanded in the following Karhunen-Lo ‘eve form:

$$\gamma(\mathbf{x},\theta) = \sum_{i=1}^{Q} \sqrt{\lambda_i} f_i(\mathbf{x}) \xi_i(\theta) \tag{5}$$

subject to the following constraint deriving from the unit variance condition imposed on $\gamma(\mathbf{x})$:

$$\sum_{i=1}^{Q} (\sqrt{\lambda_i} f_i(\mathbf{x}))^2 = 1 \tag{6}$$

Thus, it is required that we re-normalize to a unit variance as follows:

$$\gamma(\mathbf{x},\theta) = \sum_{i=1}^{Q} \frac{\sqrt{\lambda_i} f_i(x)}{\sqrt{\sum\limits_{m=1}^{Q} (\sqrt{\lambda_m} f_m(\mathbf{x}))^2}} \xi_i(\theta) \tag{7}$$

By equating the two representations of $D(\mathbf{x},\theta)$ in Eq. (1), (2) we can find the coefficients $r_i(x)$ as

$$r_i(\mathbf{x}) = \frac{p!}{\langle \Phi_i^2 \rangle} D_p(\mathbf{x}) \prod_{j=1}^{p} \frac{\sqrt{\lambda_{k(j)}} f_{k(j)}(\mathbf{x})}{\sqrt{\sum\limits_{m=1}^{Q} (\sqrt{\lambda_m} f_m(\mathbf{x}))^2}} \tag{8}$$

where p is the order of the polynomial Φ_i and k is an index on at least one of the ξ_k making up Φ_i. Note that the accuracy of the synthesized marginal probability density function depends mainly on the order M of the PC expansion, while the correlation accuracy depends on the dimension Q of $\xi(\theta)$. Finally a similar methodology may be applied in the case of generalized Polynomial Chaos (gPC) expansion [15].

This study assumes a strictly positive definite lognormal random stiffness field in conjunction with classical PCE, which admit the analytical computation of the respective coefficients. Assuming an underlying Gaussian field $g(\mathbf{x})$, the actual stiffness field is given by:

$$D(\mathbf{x}) = e^{g(\mathbf{x})} \tag{9}$$

with the following mean and variance relations:

$$\bar{D} = e^{\bar{g}} \tag{10}$$

$$\sigma_D = e^{\sigma_g} \tag{11}$$

The process $g(\mathbf{x})$ is expanded in the Karhunen-Lo ‘eve sense as:

$$g(\mathbf{x}) = \bar{g} + \sum_{i=1}^{N} g_i \xi_i = \bar{g} + \sum_{i=1}^{N} \sqrt{\lambda_i} f_i(\mathbf{x}) \xi_i \tag{12}$$

and projection into polynomial chaos yields analytical coefficients $r_i(\mathbf{x})$:

$$r_i(\mathbf{x}) = \frac{\langle e^g \Phi_i \rangle}{\langle \Phi_i^2 \rangle} = \frac{\prod_{j=1}^{p} \sqrt{\lambda_{k(j)}} f_{k(j)}(\mathbf{x})}{\langle \Phi_i^2 \rangle} e^{\bar{g} + \frac{1}{2} \sum_{j=1}^{N} g_j^2} \tag{13}$$

Fig. 1 shows how the synthesized marginal probability density function using this methodology converges to the target lognormal distribution for a case of COV = 30% for an increasing order of polynomial chaos approximation. Finally, Fig. 2 compares the target and approximated correlation structure for varying KL dimensionality.

2.2. Shear strength

In the case of a non-Gaussian shear strength random field $S_u(\mathbf{x}, \theta)$, the above methodology may be applied considering the two fields to be independent of each other. Alternatively, for computational efficiency and since the stability of the simulation remains unaffected, one may choose to approximate the shear strength field simply by KLE as follows:

$$S_u(\mathbf{x}, \theta) = \bar{S_u}(\mathbf{x}) + \sum_{i=1}^{N} \sqrt{\lambda_i} f_i(\mathbf{x}) \xi_i(\theta) \tag{14}$$

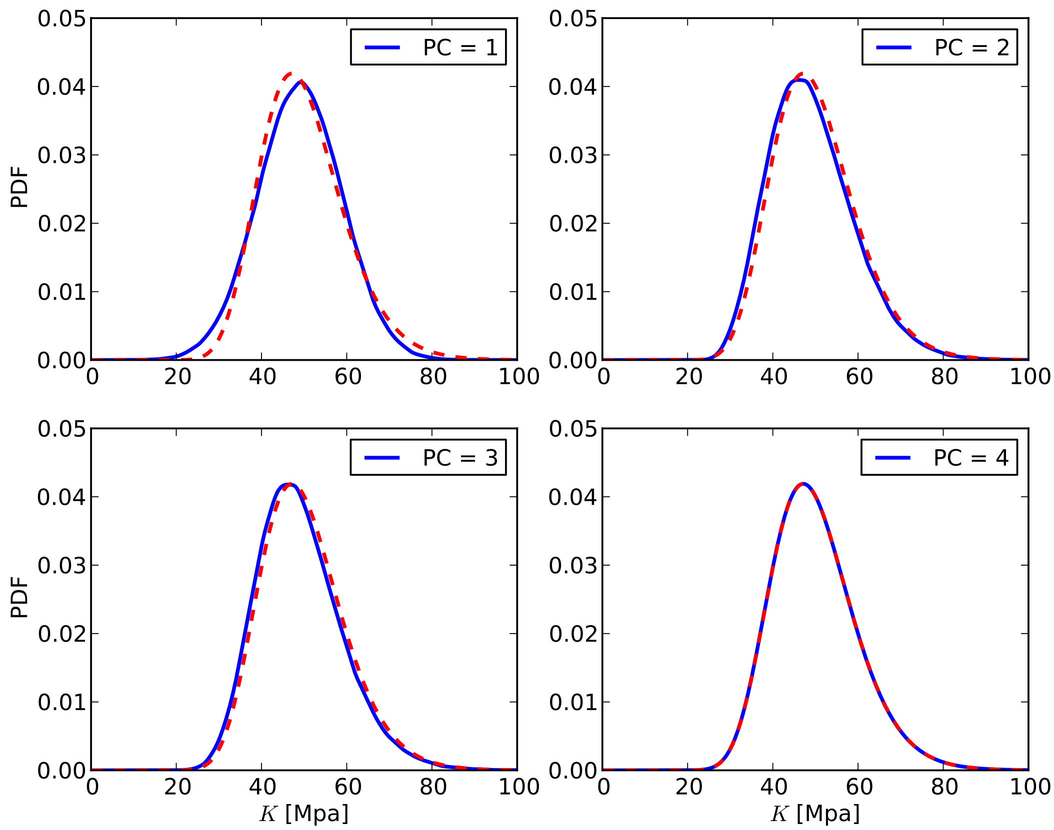

Figure 1: Convergence of the PC approximation (blue) to the target (red) lognormal distribution.

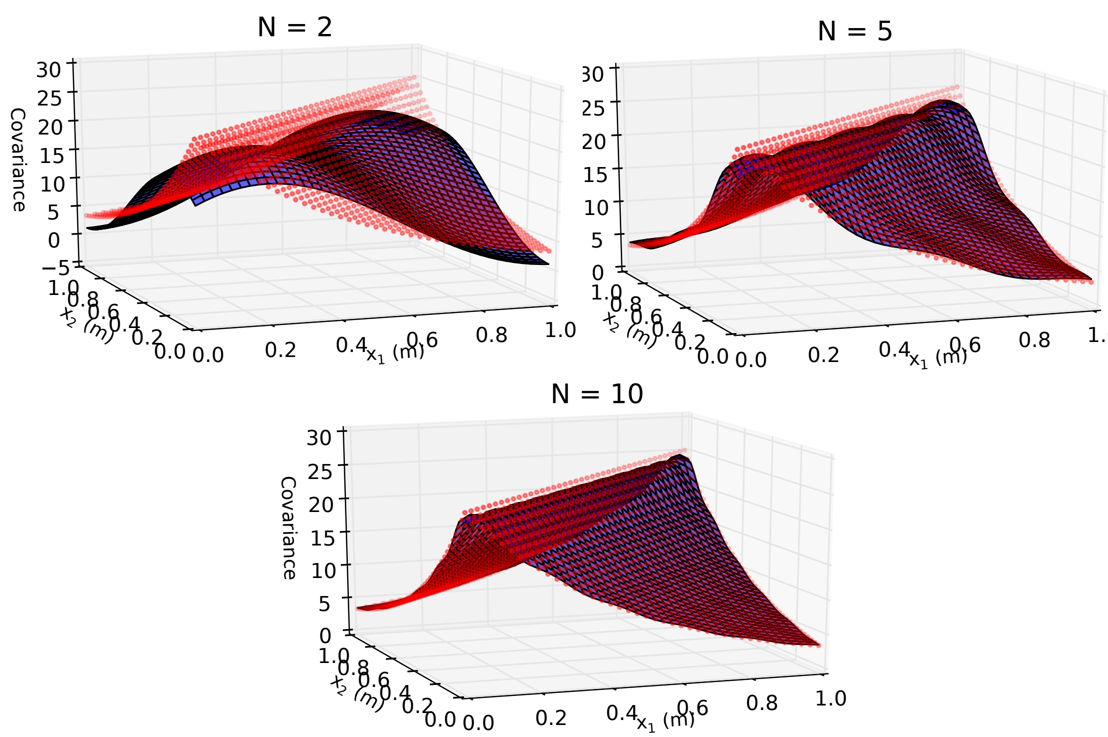

Figure 2: Comparing the approximated (blue) to the target (red) correlation structure.

by considering the following Fredholm integral equation of the second kind [26] with the covariance function C_{S_u} as a kernel:

$$\int_D C_{S_u}(\mathbf{x}_1, \mathbf{x}_2) f_k(\mathbf{x}_1) d\mathbf{x}_1 = \lambda_k f_k(\mathbf{x}_2) \tag{15}$$

This expansion is optimal in the sense that it is the best approximation that may be achieved in the $L_2(D) \otimes L_2(\Omega)$ norm.

In some cases (e.g. triangular, exponential kernel) the above eigenproblem may be solved analytically, but in the general case a numerical approximation scheme is required. In that sense, a number of methods have been applied including FEM [11], wavelet-Galerkin [27], $\mathcal{H}$-matrices [28] and meshless methods [29].

In a standard finite element setting, each eigenfunction f_k of the kernel is approximated as:

$$f_k(\mathbf{x}) = \sum_{i=1}^{N} d_{ik} h_i(\mathbf{x}) \tag{16}$$

Utilizing the above representation and requiring the error to be orthogonal to the approximating space, transforms Eq. 15 to the following weak form:

$$\sum_{i=1}^{N} d_{ik} \left[\int_D \int_D C_{S_u}(\mathbf{x}_1, \mathbf{x}_2) h_i(\mathbf{x}_2) h_j(\mathbf{x}_1) d\mathbf{x}_1 d\mathbf{x}_2 - \lambda_k \int_D h_i(\mathbf{x}) h_j(\mathbf{x}) d\mathbf{x} \right] = 0 \tag{17}$$

The required discretization (mesh size) depends on the correlation length describing the rate of fluctuation of the random field. It has been shown [30, 31] that 2-4 elements per correlation length are usually enough to capture the structure of the random field. In cases where the correlation structure is approximated by long-tailed kernels (e.g Gaussian), the resulting generalized "stiffness" matrix in the eigenproblem looses its sparsity resulting in an inefficient numerical solution. It is therefore common to modify (truncate) the kernels so as to increase the sparsity of the representation. Melink and Korelc [32] studied this problem in terms of numerical integration and loss of positive definiteness of the covariance matrix.

3. Spatial and Stochastic discretization of the solution

The unknown displacement random field is semi-discretized in the stochastic dimension using PCE:

$$u(\mathbf{x},\theta) = \sum_{i=0}^{P} d_i(\mathbf{x})\Psi_i[\xi_r(\theta)] \tag{18}$$

with the component $d_i(\mathbf{x})$ being further discretized in the spatial sense using finite element shape functions:

$$d_i(\mathbf{x}) = \sum_{j=1}^{N} d_{ij} N_j(\mathbf{x}) \tag{19}$$

This results in a final expression for the random displacement field:

$$u(\mathbf{x},\theta) = \sum_{i=0}^{P}\sum_{j=1}^{N} d_{ij} N_j(\mathbf{x})\Psi_i[\xi_r(\theta)] \tag{20}$$

4. Finite Element Formulation

Employing the Galerkin weak formulation of linearized static FEM [33], we have the following simplified form :

$$\sum_e \left[\int_{D_e} \nabla N_m(\mathbf{x}) D(\mathbf{x},\theta) \nabla N_n(\mathbf{x}) d\Omega \, u_m - \int_{D_e} f_m(\mathbf{x},\theta) d\Omega \right] = 0 \tag{21}$$

where $\sum_e$ denotes the assembly procedure over all finite elements of the discretized domain Ω and $f_m(\mathbf{x})$ incorporates the various elemental contributions to the global force vector.

Combining Equations 1, 20 and 21 and denoting the shape function gradients as:

$$\nabla N_n(\mathbf{x}) := B_n(\mathbf{x}) \tag{22}$$

yields:

$$\begin{aligned}\sum_e \Bigg[\int_{D_e} B_m(\mathbf{x}) \sum_{i=0}^{M} r_i(\mathbf{x}) \Phi_i[\{\xi_r(\theta)\}] B_n(\mathbf{x}) \sum_{j=0}^{P} d_{nj} \Psi_j[\xi_r(\theta)]\, d\Omega \\ - \int_{D_e} f_m(\mathbf{x},\theta) d\Omega \Bigg] = 0\end{aligned} \tag{23}$$

Taking now the Galerkin projection of the discretized equation onto each arbitrary polynomial basis of the displacement approximation $\Psi_k[\xi_r(\theta)]$:

$$\begin{aligned}\sum_e \Bigg[\int_{D_e} B_m(\mathbf{x}) \sum_{i=0}^{M} r_i(\mathbf{x}) \Phi_i[\{\xi_r(\theta)\}] B_n(\mathbf{x}) \sum_{j=0}^{P} \sum_{k=0}^{P} d_{nj} \Psi_j[\xi_r(\theta)] \Psi_k[\xi_r(\theta)]\, d\Omega \\ - \int_{D_e} \sum_{k=0}^{P} f_m(\mathbf{x},\theta) \Psi_k[\xi_r(\theta)]\, d\Omega \Bigg] = 0\end{aligned} \tag{24}$$

results in the following system of equations:

$$\sum_{n=1}^{N} \sum_{j=0}^{P} d_{nj} \sum_{k=1}^{M} b_{ijk} K_{mni} = F_m \langle \Psi_k[\{\xi_r\}] \rangle \tag{25}$$

where

$$K_{mni} = \int_D B_m(\mathbf{x}) r_i(\mathbf{x}) B_n(\mathbf{x}) d\Omega \tag{26}$$

and

$$F_m = \int_D f_m(\mathbf{x},\theta) d\Omega \tag{27}$$

Symbolic manipulations are carried out using Mathematica [34] in order to tabulate the coefficients of the tensor:

$$b_{ijk} = \langle \Phi_i[\{\xi_r\}] \Psi_j[\{\xi_r\}] \Psi_k[\{\xi_r\}] \rangle \tag{28}$$

The form of the latter induces a special block sparsity in the resulting stiffness matrix that may be exploited to develop an efficient solution scheme. Several researchers have dealt with such systems of equations arising in the context of the the spectral stochastic finite element formulation. One of the first attempts was made by Ghanem and Kruger [35] who proposed two solution procedures, a preconditioned CG method as well as a hierarchical formulation. Another iterative scheme of the family of Krylov-subspace methods that has been applied is the preconditioned MINRES [36]. In addition, researchers have developed multi-grid approaches [37] as well as incomplete block-diagonal preconditioning schemes based on the FETI-PD solver [38]. A more complete review of the methods may be found in [23].

5. Elastoplasticity

In this study, the elastoplastic behavior is treated in a spectral fashion by updating the coefficients of the stochastic approximation of the stiffness according to an underlying Fokker-Planck-Kolmogorov framework. At each integration point and orthogonal KL/PC space, the nonlinear FPK equation is solved incrementally, and an optimization procedure yields the equivalent linearized advection and diffusion terms. The updated PC coefficients are then computed based on these terms. We investigate varying approximation accuracy by restricting the number of spaces in which the integration procedure is carried out.

5.1. Formulation of FPK-based probabilistic elastoplasticity

The incremental form of spatial-average elastoplastic constitutive equation may be written as

$$\frac{d\sigma_{ij}(x_t,t)}{dt} = D_{ijkl}(x_t,t)\frac{d\epsilon_{kl}(x_t,t)}{dt} \tag{29}$$

where D_{ijkl} is the continuum stiffness tensor which can be either elastic or elasto-plastic:

$$D_{ijkl} = \begin{cases} D^{el}_{ijkl} & ; f < 0 \vee (f = 0 \wedge df < 0) \\ \\ D^{el}_{ijkl} - \dfrac{D^{el}_{ijmn}\frac{\partial U}{\partial \sigma_{mn}}\frac{\partial f}{\partial \sigma_{pq}}D^{el}_{pqkl}}{\frac{\partial f}{\partial \sigma_{rs}}D^{el}_{rstu}\frac{\partial U}{\partial \sigma_{tu}} - \frac{\partial f}{\partial q_*}r_*} & ; f = 0 \wedge df < 0 \end{cases} \tag{30}$$

according to the established Karush-Kuhn-Tucker conditions.

In the above equation, D^{el}_{ijkl} is the elastic stiffness tensor, f is the yield function, which is a function of stress σ_{ij} and internal variables q_*, while U is the plastic potential function. In its most general form, the incremental constitutive equation takes the form

$$\frac{d\sigma_{ij}(x_t,t)}{dt} = \beta_{ijkl}(\sigma_{ij}, D_{ijkl}, q_*, r_*; x_t, t)\frac{d\epsilon_{kl}(x_t,t)}{dt} \tag{31}$$

or

$$\frac{d\sigma_{ij}(x_t,t)}{dt} = \eta_{ijkl}(\sigma_{ij}, D_{ijkl}, \epsilon_{kl}(x_t,t) q_*, r_*; x_t, t) \tag{32}$$

where the stochasticity of the operator β is induced by the stochasticity of D_{ijkl}, q_*, r_*. This renders the above equation a linear/non-linear ordinary differential equation with stochastic coefficients. Similarly randomness in the forcing term (ϵ_{kl}) results in a linear/non-linear ordinary differential equation with stochastic forcing. Combining the two cases yields a linear/non-linear ordinary differential equation with stochastic coefficients and stochastic forcing. Using the Eulerian-Lagrangian form of the FPE equation [20] the above equation takes the following form in the probability density space

$$\begin{aligned}\frac{\partial P(\sigma_{ij},t)}{\partial t} = & -\frac{\partial}{\partial \sigma_{mn}}\left[\left\{\langle \eta_{mn}(\sigma_{mn}(t), D_{mnrs}, \epsilon_{rs}(t))\rangle\right.\right. \\ & + \int_0^t d\tau Cov_0\left[\frac{\partial \eta_{mn}(\sigma_{mn}(t), D_{mnrs}, \epsilon_{rs}(t))}{\partial \sigma_{ab}};\right. \\ & \left.\left.\left.\eta_{ab}(\sigma_{ab}(t-\tau), D_{abcd}, \epsilon_{cd}(t-\tau))\right]\right\} P(\sigma_{ij}(t),t)\right] \\ & +\frac{\partial^2}{\partial \sigma_{mn}\partial \sigma_{ab}}\left[\int_0^t d\tau Cov_0\left[\eta_{mn}(\sigma_{mn}(t), D_{mnrs}, \epsilon_{rs}(t));\right.\right. \\ & \left.\left.\eta_{ab}(\sigma_{ab}(t-\tau), D_{abcd}, \epsilon_{cd}(t-\tau))\right] P(\sigma_{ij}(t),t)\right] \end{aligned} \quad (33)$$

where $P(\sigma_{ij}, t)$ is the probability density of stress, $\langle\cdot\rangle$ is the expectation operator, $Cov_0[\cdot]$ is the time-ordered covariance operator and η_{ij} is a generalized random tensor operator. Details of this derivation can be found in [39]. The above equation is equivalent to the following generalized form:

$$\frac{\partial P(\sigma_{ij},t)}{\partial t} = -\frac{\partial}{\partial \sigma_{mn}}\left[N^{\sigma^{eq}}_{(1)_{mn}} P(\sigma_{ij},t) - \frac{\partial}{\partial \sigma_{ab}}\left\{N^{\sigma^{eq}}_{(2)_{mnab}} P(\sigma_{ij},t)\right\}\right] \quad (34)$$

where $N_{(1)}$ and $N_{(2)}$ are advection and diffusion coefficients respectively that are particular to the constitutive model. Given the initial and boundary conditions as well as the second-order statistics of material properties,the equation may be solved with second-order accuracy.

To account for the uncertainty in the probabilistic yielding, Jeremić and Sett [40] introduced the following equivalent advection and diffusion coefficients:

$$N^{\sigma^{eq}}_{(1)_{mn}}(\sigma_{ij}) = (1 - P[f>0])\, N^{el}_{(1)_{mn}} + P[f>0]\, N^{ep}_{(1)_{mn}} \quad (35)$$

$$N^{\sigma^{eq}}_{(2)_{mnab}}(\sigma_{ij}) = (1 - P[f>0])\, N^{el}_{(2)_{mnab}} + P[f>0]\, N^{ep}_{(2)_{mnab}} \quad (36)$$

where $(1 - P[f > 0])$ represents the probability of the material being elastic, while $P[f > 0]$ represents the probability of the material being elastoplastic. $P[f > 0]$ is obtained from the cumulative density function, rendering it an explicit function of the stress σ_{ij} as well as the internal variables q_*.

Utilizing Eq. 33, one may compute the elastic and elastoplastic coefficients addressed in Eq. 34 as:

$$N^{el}_{(1)_{mn}} = \langle D^{el}_{mnrs} \dot{\epsilon}_{rs} \rangle \tag{37}$$

$$N^{el}_{(2)_{mnab}} = t \ \mathrm{Cov}_0 \left[D^{el}_{mnrs} \dot{\epsilon}_{rs}; D^{el}_{abcd} \dot{\epsilon}_{cd} \right] \tag{38}$$

and

$$N^{ep}_{(1)_{mn}} = \langle D^{ep}_{mnrs} \dot{\epsilon}_{rs} \rangle + \int_0^t d\tau Cov_0 \left[\frac{\partial}{\partial \sigma_{ab}} \{ D^{ep}_{mnrs} \dot{\epsilon}_{rs} \}; D^{ep}_{abcd} \dot{\epsilon}_{cd} \right] \tag{39}$$

$$N^{ep}_{(2)_{mnab}} = \int_0^t d\tau Cov_0 \left[D^{ep}_{mnrs}(t) \dot{\epsilon}_{rs}; D^{ep}_{abcd}(t - \tau) \dot{\epsilon}_{cd} \right] \tag{40}$$

The evolution of an internal variable $\mathbf{q}$ of the model is handled through a coupled FPK equation of the form:

$$\frac{\partial \tilde{P}(q_i, t)}{\partial t} = -\frac{\partial}{\partial q_m} \left[N^{q^{eq}}_{(1)_m}(\sigma_{mn}, q_m) \tilde{P}(q_i, t) - \frac{\partial}{\partial q_n} \left\{ N^{q^{eq}}_{(2)_{mn}}(\sigma_{mn}, q_m) \tilde{P}(q_i, t) \right\} \right] \tag{41}$$

The advection and diffusion coefficients in the above equation are given similarly to Eq. 35 and 35 but with no contributions of any 'elastic' state:

$$N^{q^{eq}}_{(1)_m}(\sigma_{ij}, q_i) = P[f > 0] \, N^{q^{ep}}_{(1)_m} \tag{42}$$

$$N^{q^{eq}}_{(2)_{mn}}(\sigma_{ij}, q_i) = P[f > 0] \, N^{q^{ep}}_{(2)_{mn}} \tag{43}$$

The elastoplastic components of the equivalent advection and diffusion terms are functions of the so-called loading index or plastic multiplier L and the rates of evolution of the internal variables r_i:

$$N^{q^{ep}}_{(1)_m} = \langle Lr_i \rangle + \int_0^t d\tau \mathrm{Cov}_0 \left[\frac{\partial}{\partial q_j} Lr_i(t); Lr_j(t-\tau) \right] \tag{44}$$

$$N^{q^{ep}}_{(2)_{mn}} = \int_0^t d\tau \mathrm{Cov}_0 \left[Lr_i(t); Lr_j(t-\tau) \right] \tag{45}$$

where L may be expressed as:

$$L = \frac{\dfrac{\partial f}{\partial \sigma_{ot}} D^{el}_{ijot} \dot{\epsilon}_{ij}}{\dfrac{\partial U}{\partial \sigma_{ab}} D^{el}_{abcd} \dfrac{\partial f}{\partial \sigma_{cd}} - \dfrac{\partial f}{\partial q_m} r_m} \tag{46}$$

5.2. Linearization for stiffness update

The constitutive integration of the FPK-based plasticity model cannot directly provide the updated generalized stiffness at the finite element level. Therefore, a numerical scheme is required in order to compute the stiffness in a PC expansion form as per Eq. 1. In this study we assume an equivalent linear FPK equation involving the updated PC coefficients which are deduced through a least-squares optimization procedure.

For each orthogonal KL/PC space s, Eq. 34 applies with the advection and diffusion coefficients taking the form:

$$N^{s^{eq}}_{(1)_{mn}}(\sigma^s_{ij}, \mathbf{x}) = (1 - P[f > 0])\, N^{el}_{(1)_{mn}} + P[f > 0]\, N^{ep}_{(1)_{mn}} \tag{47}$$

$$N^{s^{eq}}_{(2)_{mnab}}(\sigma^s_{ij}, \mathbf{x}) = (1 - P[f > 0])\, N^{el}_{(2)_{mnab}} + P[f > 0]\, N^{ep}_{(2)_{mnab}} \tag{48}$$

For the purposes of this study, let us consider an isotropic linear elastic - Mises isotropic hardening model and derive the equivalent advection and diffusion coefficients for this case. The isotropic linear elasticity tensor in

Eq. 30 reads:

$$D^{el}_{ijkl} = G\delta_{ik}\delta_{jl} + \left(K - \frac{2}{3}G\right)\delta_{ij}\delta_{kl} \tag{49}$$

where K and G denote the bulk and shear modulus respectively and are represented as random fields (see for example Eq. 1).

The elastoplastic continuum tangent tensor in Eq. 30 is given in the following general form:

$$D^{ep}_{ijkl} = G\delta_{ik}\delta_{jl} + \left(K - \frac{2}{3}G\right)\delta_{ij}\delta_{kl} - \frac{A_{ij}A^*_{kl}}{B + K_P} \tag{50}$$

The Mises linear hardening yield function is written as:

$$f = \sqrt{J_2} - k = \sqrt{\frac{1}{2}s_{ij}s_{ij}} - k \tag{51}$$

Under the assumption of associated flow rule we have:

$$\frac{\partial f}{\partial \sigma_{ij}} = \frac{\partial U}{\partial \sigma_{ij}} \tag{52}$$

which results in the following symmetry:

$$A_{ij} = A^*_{ij} = D^{el}_{ijkl}\frac{\partial f}{\partial \sigma_{kl}} \tag{53}$$

After some algebraic manipulations, one can easily derive:

$$A_{ij} = \frac{G}{\sqrt{J_2}}s_{ij} \qquad B = G \tag{54}$$

The plastic modulus K_P is computed here on the basis of a deterministic hardening rule in terms of the equivalent plastic strain:

$$k = k(e^p_{eq}) \tag{55}$$

After imposing the consistency condition, we have:

$$K_P = -\frac{\partial f}{\partial k}\bar{k} = -\frac{1}{\sqrt{3}}\frac{\partial f}{\partial k}\frac{dk}{de^p_{eq}}\frac{\partial f}{\partial\sqrt{J_2}} = \frac{1}{\sqrt{3}}\frac{dk}{de^p_{eq}} \tag{56}$$

Combining Equations 35-40 and 49- 50, we can derive the final coefficients of the FPK constitutive rate equation as:

$$
\begin{aligned}
N^{s^{eq}}_{(1)_{mn}} &= (1-P[f>0])\left\langle\left[G\delta_{mr}\delta_{ns}+\left(K-\frac{2}{3}G\right)\delta_{mn}\delta_{rs}\right]\dot{\epsilon}_{rs}(t)\right\rangle \\
&+P[f>0]\left\langle\left[G\delta_{mr}\delta_{ns}+\left(K-\frac{2}{3}G\right)\delta_{mn}\delta_{rs}-\right.\right. \\
&\left.\left.\frac{1}{G+\frac{1}{\sqrt{3}}\frac{dk}{de^p_{eq}}}\left(\frac{G}{\sqrt{J_2}}\right)^2 s^s_{ij}(t)s^s_{kl}(t)\right]\dot{\epsilon}_{rs}(t)\right\rangle \\
&+\int_0^t d\tau Cov_0\left[\frac{\partial}{\partial\sigma^s_{ab}}\left\{\left[G\delta_{mr}\delta_{ns}+\left(K-\frac{2}{3}G\right)\delta_{mn}\delta_{rs}\right.\right.\right. \\
&\left.\left.-\frac{1}{G+\frac{1}{\sqrt{3}}\frac{dk}{de^p_{eq}}}\left(\frac{G}{\sqrt{J_2}}\right)^2 s^s_{ij}(t)s^s_{kl}(t)\right]\dot{\epsilon}_{rs}(t)\right\}; \\
&\left[G\delta_{ac}\delta_{bd}+\left(K-\frac{2}{3}G\right)\delta_{ab}\delta_{cd}-\right. \\
&\left.\left.\frac{1}{G+\frac{1}{\sqrt{3}}\frac{dk}{de^p_{eq}}}\left(\frac{G}{\sqrt{J_2}}\right)^2 s^s_{ab}(t-\tau)s^s_{cd}(t-\tau)\right]\dot{\epsilon}_{cd}(t-\tau)\right]
\end{aligned}
\tag{57}
$$

$$
\begin{aligned}
N^{s^{eq}}_{(2)_{mnab}} \quad = \quad & (1 - P[f > 0])\, t \ \mathrm{Cov}_0 \Bigg[\Bigg\{ G\delta_{mr}\delta_{ns} + \left(K - \frac{2}{3}G\right)\delta_{mn}\delta_{rs} \\
& - \frac{1}{G + \frac{1}{\sqrt{3}}\frac{dk}{de^p_{eq}}} \left(\frac{G}{\sqrt{J_2}}\right)^2 s^s_{ij}(t) s^s_{kl}(t) \Bigg\} \dot{\epsilon}_{rs}(t); \\
& \Bigg[G\delta_{ac}\delta_{bd} + \left(K - \frac{2}{3}G\right)\delta_{ab}\delta_{cd} - \\
& \frac{1}{G + \frac{1}{\sqrt{3}}\frac{dk}{de^p_{eq}}} \left(\frac{G}{\sqrt{J_2}}\right)^2 s^s_{ab}(t) s^s_{cd}(t) \Bigg] \dot{\epsilon}_{cd}(t) \Bigg] \\
& + P[f > 0] \int_0^t d\tau Cov_0 \Bigg[\Bigg\{ G\delta_{mr}\delta_{ns} + \left(K - \frac{2}{3}G\right)\delta_{mn}\delta_{rs} \\
& - \frac{1}{G + \frac{1}{\sqrt{3}}\frac{dk}{de^p_{eq}}} \left(\frac{G}{\sqrt{J_2}}\right)^2 s^s_{ij}(t) s^s_{kl}(t) \Bigg\} \dot{\epsilon}_{rs}(t); \\
& \Bigg\{ G\delta_{ac}\delta_{bd} + \left(K - \frac{2}{3}G\right)\delta_{ab}\delta_{cd} - \\
& \frac{1}{G + \frac{1}{\sqrt{3}}\frac{dk}{de^p_{eq}}} \left(\frac{G}{\sqrt{J_2}}\right)^2 s^s_{ab}(t-\tau) s^s_{cd}(t-\tau) \Bigg\} \dot{\epsilon}_{cd}(t-\tau) \Bigg]
\end{aligned} \tag{58}
$$

Next let us consider a linearized FPK equation for the stress corresponding to the orthogonal space s at the k$^{\text{th}}$-step in the following form:

$$
\frac{\partial P^{lin}(\sigma^s_{ij}, t)}{\partial t} = -N^{s^{lin}}_{(1)_{mn}} \frac{\partial P(\sigma^s_{ij}, t)}{\partial \sigma^s_{mn}} + N^{s^{lin}}_{(2)_{mnab}} \frac{\partial^2 P(\sigma^s_{ij}, t)}{\partial \sigma^s_{mn} \sigma^s_{ab}} \tag{59}
$$

where the linearized advection and diffusion coefficients are given by:

$$\begin{aligned} N^{s^{lin}}_{(1)_{mn}} &= r^{s(k)}_{mnab} \sum_{i=0}^{P} \langle \Phi_i \Psi_s \rangle \\ & \quad \frac{1}{2\Delta t} \sum_{j=1}^{N} \left[N_{j,b}(\mathbf{x}) \Delta d^{k-1}_{ija} + N_{j,a}(\mathbf{x}) \Delta d^{k-1}_{ijb} \right] \end{aligned} \tag{60}$$

$$\begin{aligned} N^{s^{lin}}_{(2)_{mnab}} &= t \, (r^{s(k)}_{mnab})^2 \sum_{i=0}^{P} \mathrm{Var} \left[\Phi_i \Psi_s \right] \\ & \quad \frac{1}{4\Delta t^2} \left[N_{j,b}(\mathbf{x}) \Delta d^{k-1}_{ija} + N_{j,a}(\mathbf{x}) \Delta d^{k-1}_{ijb} \right]^2 \end{aligned} \tag{61}$$

In an explicit scheme, the strain increment at the (k-1)$^{\mathrm{th}}$ step is utilized, while the fourth-order tensor valued PC coefficient $r^{s(k)}_{mnab}$ is unknown. Depending on the specific constitutive model, the above equations may be simplified to include scalar PC coefficients and deterministic bases in an appropriate tensor format. Combining Equations 34 and 59, one ends up with an over-determined residual system of equations in terms of the unknown coefficients at time step k:

$$R_i(r^{s(k)}_{mnab}) = \frac{\partial P^{lin}(\boldsymbol{\sigma}^s_i, t)}{\partial t} - \frac{\partial P(\boldsymbol{\sigma}^s_i, t)}{\partial t} = 0, \quad i = 1, \ldots, N \tag{62}$$

Each equation corresponds to a single point in the stress domain and the system of equations may be solved in the least squares sense using for example the Levenberg - Marquardt algorithm [41].

5.3. Varying order of accuracy

The outlined linearization scheme is accurate to the order of the KL/PC approximation of the stiffness. However, one can restrict the accuracy of the method to second order with significant computational time savings, by considering the integration of a single FPK equation at any point in the discretized domain. This is achieved by considering the total stress $\boldsymbol{\sigma}$ rather than each KL/PC stress component $\boldsymbol{\sigma}^s$. The linearized equation becomes:

$$\frac{\partial P^{lin}(\sigma_{ij},t)}{\partial t} = -N^{lin}_{(1)}\frac{\partial P(\sigma_{ij},t)}{\partial \sigma_{mn}} + N^{lin}_{(2)}\frac{\partial^2 P(\sigma_{ij},t)}{\partial \sigma_{mn}\sigma_{ab}} \tag{63}$$

where:

$$\begin{aligned} N^{lin}_{(1)} &= \sum_{s=0}^{M} r^{s(k)}_{mnab}\sum_{i=0}^{P}\langle \Phi_i \Psi_s\rangle \\ &\quad \frac{1}{2\Delta t}\sum_{j=1}^{N}\left[N_{j,b}(\mathbf{x})\Delta d^{k-1}_{ija} + N_{j,a}(\mathbf{x})\Delta d^{k-1}_{ijb}\right] \end{aligned} \tag{64}$$

$$\begin{aligned} N^{lin}_{(2)}(r^k_s,\mathbf{x}) &= t\sum_{s=0}^{M}(r^{s(k)}_{mnab})^2\sum_{i=0}^{P}\mathrm{Var}\left[\Phi_i\Psi_s\right] \\ &\quad \frac{1}{4\Delta t^2}\left[N_{j,b}(\mathbf{x})\Delta d^{k-1}_{ija} + N_{j,a}(\mathbf{x})\Delta d^{k-1}_{ijb}\right]^2 \end{aligned} \tag{65}$$

Again the resulting system of equations is generally over-determined and may be solved using least-squares techniques. Due to the form of the FPK constitutive integrator, we do not expect higher order accuracy in the linearized tangent stiffness. Indeed, studying the above system, it is evident that only 2 coefficients may be determined, while the polynomial chaos coefficients that correspond to third and higher order are dependent (negatively correlated) variables. It is proposed that the higher order coefficients retain their elastic values in order to achieve higher order accuracy during elastic loading or unloading.

In a more general sense, one can choose the number of orthogonal KL/PC spaces in which the integration procedure is carried out based on *a posteriori* error estimation techniques. However, a study of the accuracy of such a technique is out of the scope of this study.

6. Numerical illustrations

In this last section, the proposed framework is applied to the static loading of a shear beam representing a one-dimensional soil column under undrained conditions. The simplified numerical model is shown in Fig. 3. Two different cases are considered to test the methodology against parameters that differentiate the contribution of each orthogonal space, the evolution of the stress PDF as well as the global response (Table 1).

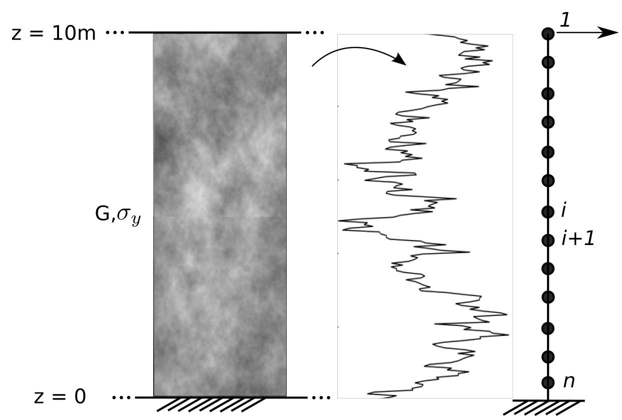

Figure 3: Realization of the stiffness random field and simplified numerical model.

Case	l_c^{G,σ_y}	$\langle G\rangle$	COV_G	$\langle\sigma_y\rangle$	COV_{σ_y}	k_{hard}	n_{KL}	m_{PC_d}	s_{PC_k}
1	0.2	50	0.4	0.8	0.1	0	2	2	2
2	1	50	0.1	0.8	0.4	10	2	2	2

Table 1: Parameters for the examples in this study

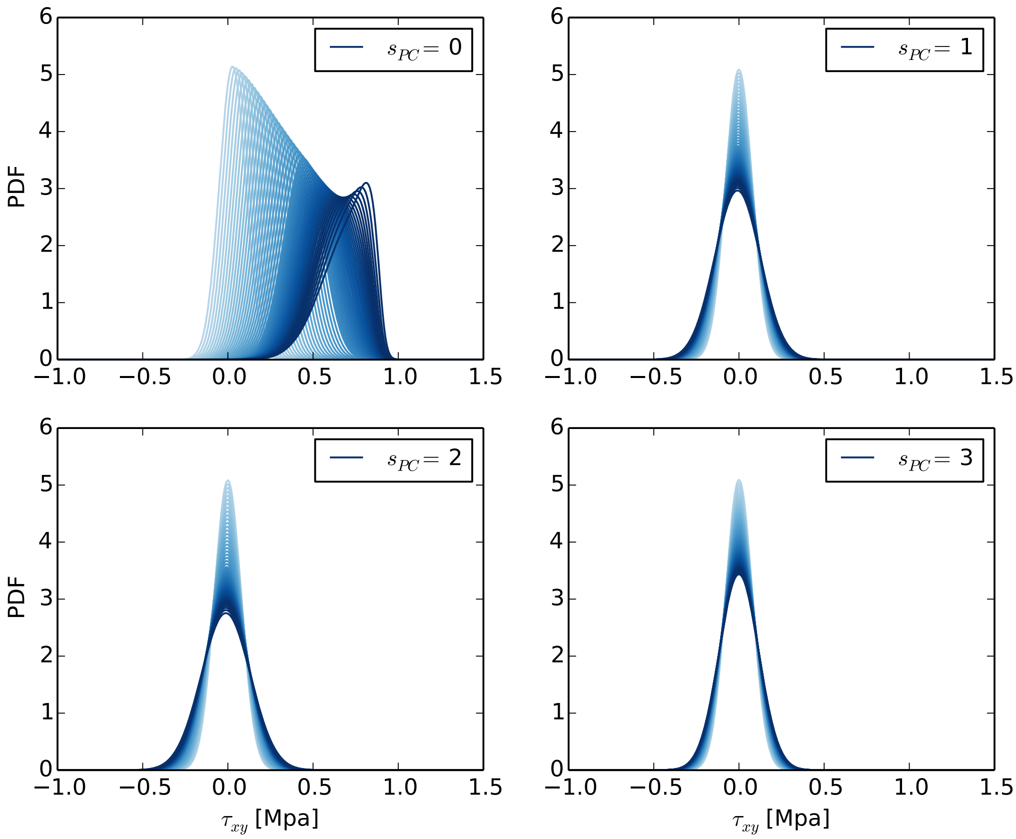

Figure 4: Evolution of the PDF of shear stress at the first 4 orthogonal KL/PC spaces (Case 1).

Fig. 4 shows the evolution of the PDF of stress at the first 4 orthogonal Kl/PC spaces at the top of the shear beam for *case 1*. Due to the small correlation length and large coefficient of variation of the shear modulus, all stress spaces are active. The evolution of the PDF in the mean shear stress space is initially diffusive and then sharpens in a quick transition to the elastoplastic regime. On the other hand, the remaining stress spaces exhibit

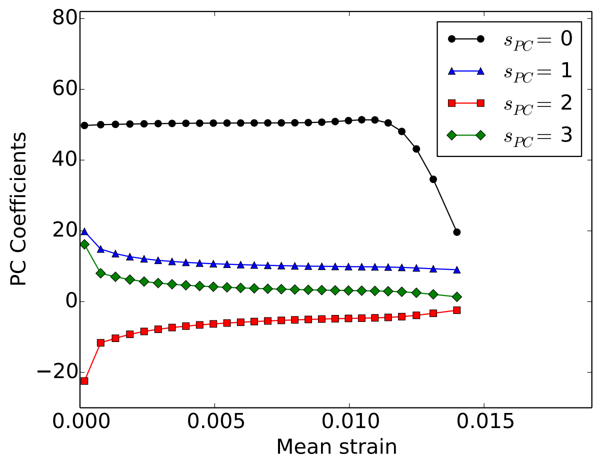

Figure 5: Evolution of PC coefficients of the linearized random shear stiffness (Case 1).

mostly diffusion. At the same spatial point, Fig.5 shows the evolution of PC coefficients derived by means of the proposed linearization procedure. After a few steps, the optimization procedure has converged and the values of the coefficients remain almost constant until their sharp decline towards zero at the end of loading. The evolution of the profile of coefficients (along the depth of the shear beam) is given in Fig. 6, where the shape of the initial profile (light color) is determined by the underlying KL eigenvectors. It is evident that the aforementioned profile values ultimately tend to zero due to the elastic-perfectly plastic nature of the model. Finally, the global force-(mean ± std.dev) displacement response at the top is shown in Fig. 7, where we can identify a sharp transition to a perfectly plastic response.

Case 2 involves a more uncertain initial yield strength along with a deterministic hardening modulus, which results in the characteristic evolution of the PDF of shear strength at the top as shown in Fig. 8. Due to the large

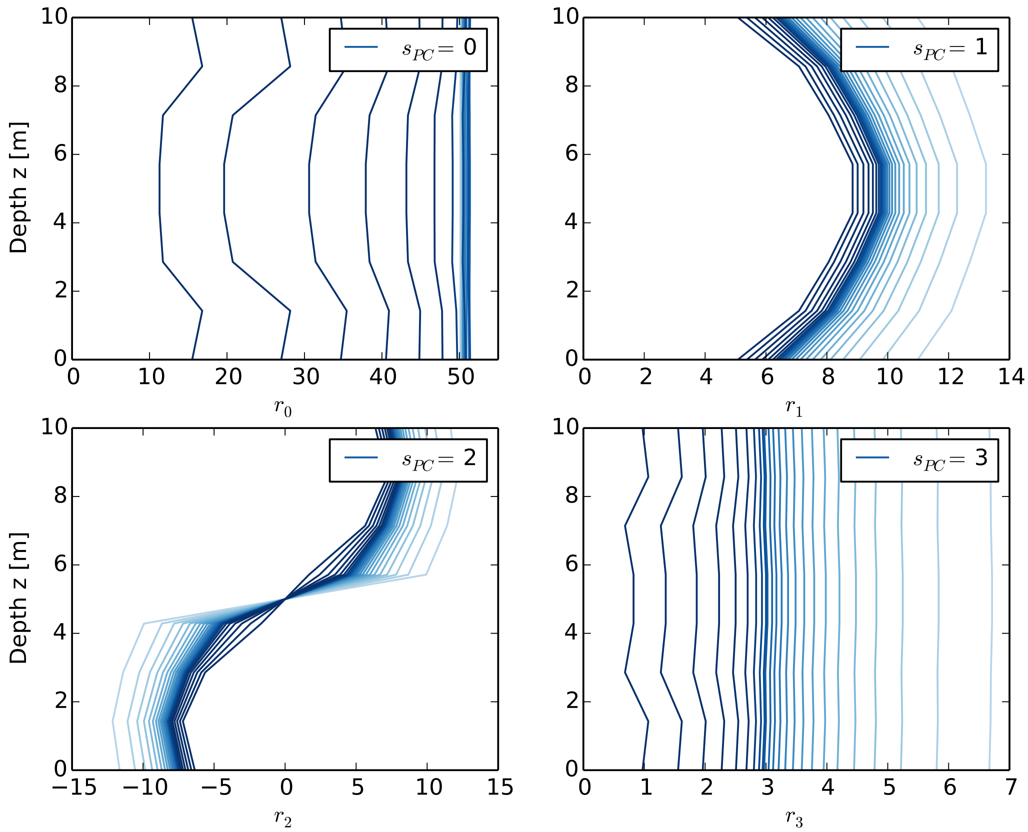

Figure 6: Evolution of the profile of PC coefficients of the linearized random shear stiffness along the depth of the shear beam (Case 1).

correlation length and small coefficient of variation of the shear modulus, the mean stress space is mostly active as well as the first stress space, which again is mostly diffusive. The associated values of the PC coefficients are shown in Fig. 9, which shows a smooth decline of the governing coefficient due to the wide range of the elastoplastic transition. Fig. 10 shows the evolution of the profile of the PC coefficients of the linearized random stiffness similar

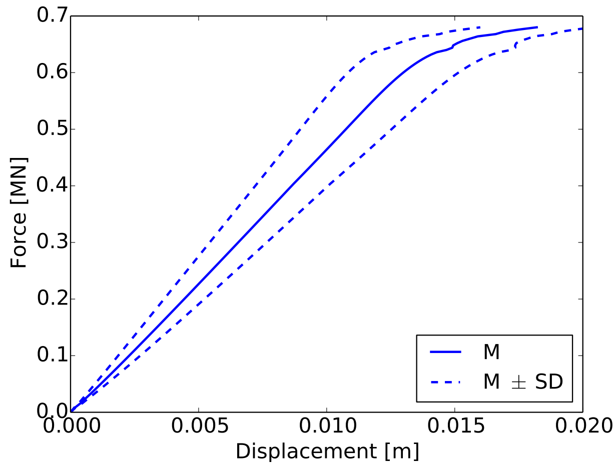

Figure 7: Force- mean ± std. dev. of displacement plot at the top of the shear column (Case 1).

to *Case 1*. Finally the global force-displacement response at the top of the shear beam is shown in Fig. 11, where we can identify a smooth transition to a linear hardening response.

7. Conclusions

We have proposed a numerical technique to solve inelastic random boundary value problems based on stochastic Galerkin techniques and a nonlocal Fokker-Planck-Kolmogorov plasticity framework. It relies on a general linearization procedure that couples any functional representation of parametric uncertainty with an underlying advection-diffusion model describing its evolution. Being an intrusive framework it has the potential for higher convergence rates than conventional non-intrusive techniques, especially when combined with sparse PC representations and efficient FPK solution methods.

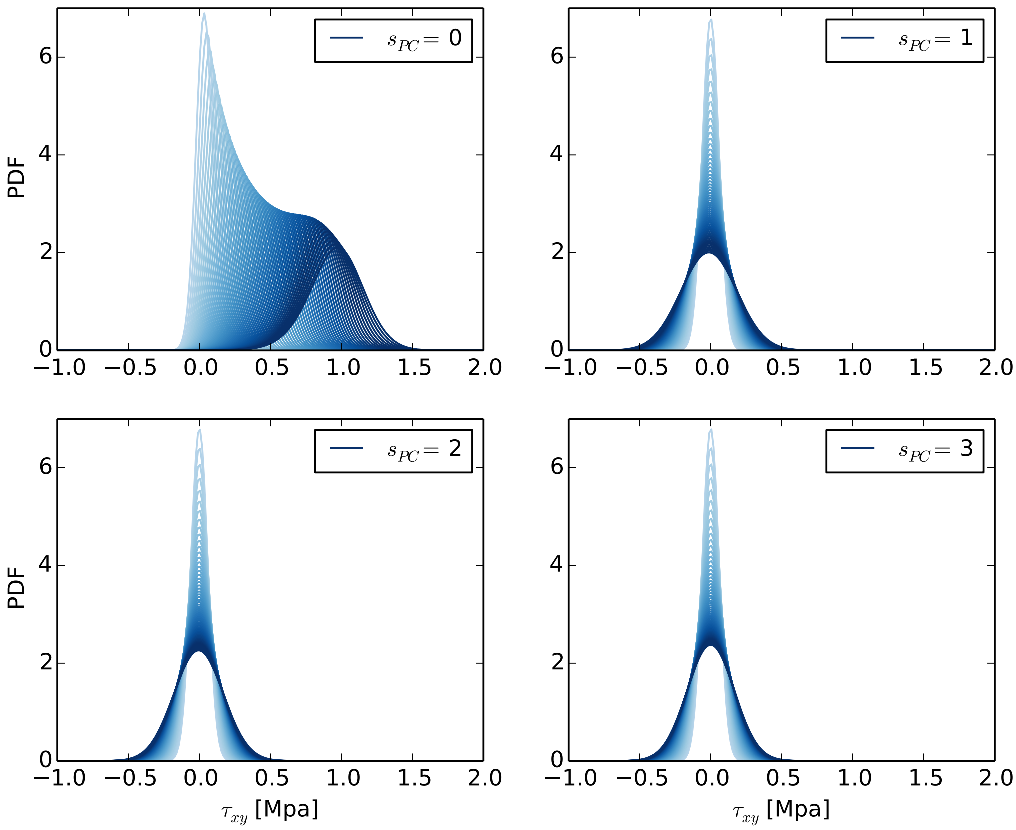

Figure 8: Evolution of the PDF of shear stress at the first 4 orthogonal KL/PC spaces (Case 2).

An additional advantage of the method is its potential to balance accuracy and computation based on error estimates.

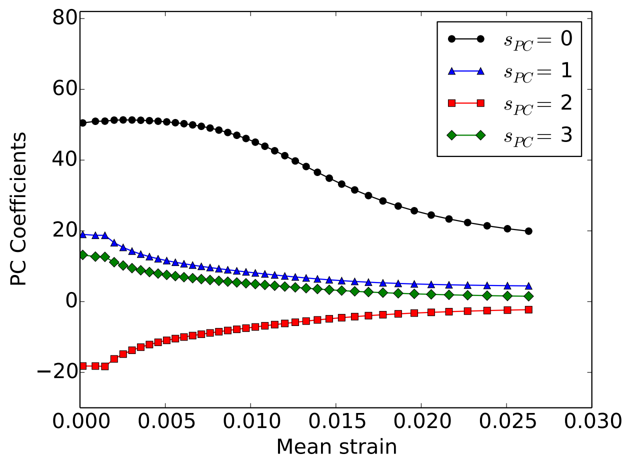

Figure 9: Evolution of PC coefficients of the linearized random shear stiffness (Case 2).

8. Acknowledgements

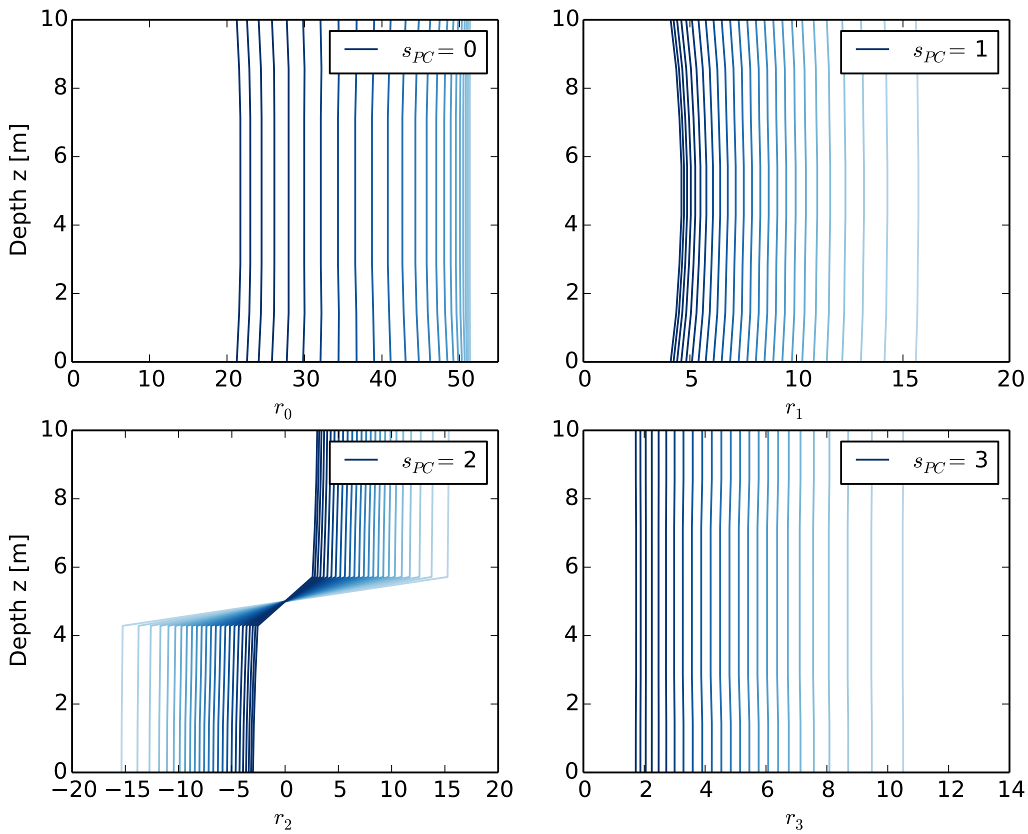

Figure 10: Evolution of the profile of PC coefficients of the linearized random shear stiffness along the depth of the shear beam (Case 2).

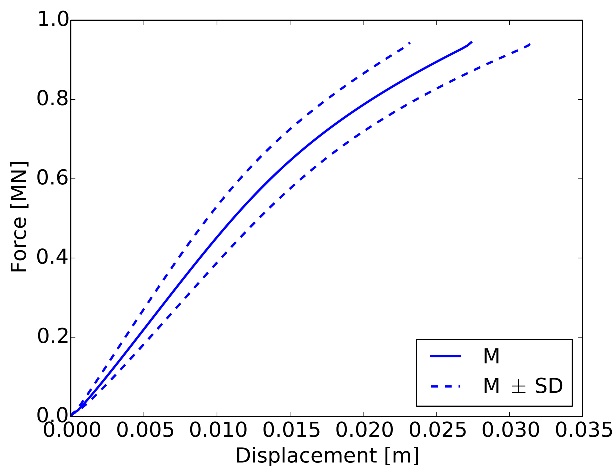

Figure 11: Force- mean ± std. dev. of displacement plot at the top of the shear column (Case 2).

References

References

[1] G. A. Fenton, Random field modeling of cpt data, ASCE Journal of Geotechnical and Geoenvironmental Engineering 125 (1999) 486–498.

[2] K.-K. Phoon, F. H. Kulhawy, Characterization of geotechnical variability, Canadian Geotechnical Journal 36 (1999) 612–624.

[3] A. L. Jones, S. L. Kramer, P. Arduino, Estimation of Uncertainty in Geotechnical Properties for Performance-Based Earthquake Engineering, Technical Report PEER 2002/16, Pacific Earthquake Engineering Research Center, 2002.

[4] G. I. Schüeller, A state-of-the-art report on computational stochastic mechanics, Probabilistic Engineering Mechanics 12 (1997) 197–321.

[5] H. G. Matthies, C. E. Brenner, C. G. Bucher, C. Guedes Soares, Uncertainties in probabilistic numerical analysis of structures and soilds - stochastic finite elements, Structural Safety 19 (1997) 283–336.

[6] I. Babuska, N. F, R. Tempone, A stochastic collocation method for elliptic partial differential equations with random input data, SIAM J. Numer. Anal. 45 (2007) 1005–1034.

[7] D. Xiu, Fast numerical methods for stochastic computations, Commun. Comput. Physics 5 (2008) 242–272.

[8] L. Giraldi, A. Litvinenko, D. Liu, H. Matthies, A. Nouy, To be or not to be intrusive? the solution of parametric and stochastic equations—the

"plain vanilla" galerkin case, SIAM J. Sci. Comput. 36 (2014) A2720–A2744.

[9] A. Keese, A Review of Recent Developments in the Numerical Solution of Stochastic Partial Differential Equations (Stochastic Finite Elements), Scientific Computing 2003-06, Deapartment of Mathematics and Computer Science, Technical University of Braunschweig, Brunswick, Germany, 2003.

[10] H. Matthies, Uncertainty Quantification with Stochastic Finite Elements, Wiley, 2004.

[11] R. G. Ghanem, P. D. Spanos, Stochastic Finite Elements: A Spectral Approach, Springer-Verlag, 1991. (Reissued by Dover Publications, 2003).

[12] N. Wiener, The homogeneous chaos, American Journal of Mathematics 60 (1938) 897–936.

[13] M. K. Deb, I. M. Babuska, J. T. Oden, Solution of stochastic partial differential equations using Galerkin finite element techniques, Computer Methods in Applied Mechanics and Engineering 190 (2001) 6359–6372.

[14] H. G. Matthies, A. Keese, Galerkin methods for linear and nonlinear elliptic stochastic partial differential equations, Computational Methods in Applied Mechanics and Engineering 194 (2005) 1295–1331.

[15] D. Xiu, G. E. Karniadakis, The wiener–askey polynomial chaos for stochastic differential equations, SIAM Journal on Scientific Computing 24 (2002) 619–644.

[16] H. G. Matthies, A. Litvinenko, O. Pajonk, B. V. Rosić, E. Zander, Parametric and uncertainty computations with tensor product representations, in uncertainty quantification in scientific computing, IFIP Advances in Information and Communication Technology 377 (2012) 139–150.

[17] A. Nouy, A. Cléent, eXtended stochastic finite element method for the numerical simulation of heterogeneous materials with random material interfaces, International Journal for Numerical Methods in Engineering Published online in Wiley Online Library (wileyonlinelibrary.com) (2010) 1–33.

[18] M. Anders, M. Hori, Three-dimensional stochastic finite element method for elasto-plastic bodies, International Journal for Numerical Methods in Engineering 51 (2001) 449–478.

[19] B. Jeremić, K. Sett, M. L. Kavvas, Probabilistic elasto-plasticity: formulation in 1D, Acta Geotechnica 2 (2007) 197–210.

[20] M. L. Kavvas, Nonlinear hydrologic processes: Conservation equations for determining their means and probability distributions, Journal of Hydrologic Engineering 8 (2003) 44–53.

[21] B. Jeremić, High fidelity modeling and simulation of sfs interaction: energy dissipation by design, in: R. P. Orense, N. Chouw, M. Pender (Eds.), Soil-Foundation-Structure Interaction, CRC Press, Taylor & Francis Group, 2010, pp. 125–132.

[22] K. Sett, B. Jeremić, M. L. Kavvas, Stochastic elastic-plastic finite elements, Computer Methods in Applied Mechanics and Engineering 200 (2011) 997–1007.

[23] B. Rosić, A Review of Computational Stochastic Elastoplasticity, Technical Report Informatikbericht Nr. 2008-08, Technische Universität Braunschweig, 2009.

[24] S. Sakamoto, R. Ghanem, Polynomial chaos decomposition for the simulation of non-gaussian nonstationary stochastic processes, Journal of Engineering Mechanics 128 (2002) 190–201.

[25] F. Benth, J. Gjerde, Convergence rates for finite element approximations for stochastic partial differential equations, Stoch. Stoch. Rep. 63 (1998) 313–326.

[26] R. Courant, D. Hilbert, Methods of Mathematical Physics, Wiley, 1989.

[27] K. Phoon, S. Huang, S. Quek, Implementation of Karhunen–Loeve expansion for simulation using a wavelet–Galerkin scheme, Probabilistic Engineering Mechanics 17 (2002) 293–303.

[28] B. Khoromskij, A. Litvinenko, H. Matthies, Application of hierarchical matrices for computing the karhunenlove expansion, Computing 84 (2009) 49–67.

[29] S. Rahman, H. Xu, A meshless method for computational stochastic mechanics, Int. J. Comput. Meth. Eng. Sc. Mech. 6 (2005) 41–58.

[30] A. Der Kiureghian, B. J. Ke, The stochastic finite element method in structural reliability, Journal of Probabilistic Engineering Mechanics 3 (1988) 83–91.

[31] C.-C. Li, A. Der Kiureghian, Optimal discretization of random fields, Journal of Engineering Mechanics, ASCE 119 (1993) 1136–1154.

[32] T. Melink, J. Korelc, Stability of karhunenlove expansion for the simulation of gaussian stochastic fields using galerkin scheme, Probabilistic Engineering Mechanics 37 (2014) 7 – 15.

[33] T. Hughes, The Finite Element Method ; Linear Static and Dynamic Finite Element Analysis, Prentice Hall Inc., 1987.

[34] Wolfram Research Inc., Mathematica Version 5.0, Wolfram Research Inc., Champaign, Illonois, 2003.

[35] R. Ghanem, R. M. Kruger, Numerical solution of spectral stochastic finite element systems, Computer Methods in Applied Mechanics and Engineering 129 (1996) 289 – 303.

[36] E. Ullmann, Solution strategies for stochastic finite element discretizations, Doctoral dissertation, TU Bergakademie Freiberg, 2008.

[37] O. L. Maitre, O. M. Knio (2010).

[38] D. Ghosh, P. Avery, C. Farhat, A feti-preconditioned conjugate gradient method for large-scale stochastic finite element problems, International Journal for Numerical Methods in Engineering 80 (2009) 914–931.

[39] B. Jeremić, K. Sett, M. L. Kavvas, Probabilistic elasto-plasticity: Formulation in 1–D, Acta Geotechnica 2 (2007) 197–210.

[40] B. Jeremić, K. Sett, On probabilistic yielding of materials, Communications in Numerical Methods in Engineering 25 (2009) 291–300.

[41] K. Levenberg, A method for the solution of certain non-linear problems in least squares, Quart. Appl. Math. 2 (1944) 164–168.